



This discussion paper is/has been under review for the journal Atmospheric Chemistry and Physics (ACP). Please refer to the corresponding final paper in ACP if available.

# Examining the effects of anthropogenic emissions on isoprene-derived secondary organic aerosol formation during the 2013 Southern Oxidant and Aerosol Study (SOAS) at the Look Rock, Tennessee, ground site

S. H. Budisulistiorini<sup>1,6</sup>, X. Li<sup>1</sup>, S. T. Bairai<sup>2,\*</sup>, J. Renfro<sup>3</sup>, Y. Liu<sup>4</sup>, Y. J. Liu<sup>4</sup>, K. A. McKinney<sup>4</sup>, S. T. Martin<sup>4</sup>, V. F. McNeill<sup>5</sup>, H. O. T. Pye<sup>6</sup>, A. Nenes<sup>7,8,9</sup>, M. E. Neff<sup>10</sup>, E. A. Stone<sup>10</sup>, S. Mueller<sup>2,\*\*</sup>, C. Knote<sup>11</sup>, S. L. Shaw<sup>12</sup>, Z. Zhang<sup>1</sup>, A. Gold<sup>1</sup>, and J. D. Surratt<sup>1</sup>

<sup>1</sup>Department of Environmental Sciences and Engineering, Gillings School of Global Public Health, The University of North Carolina at Chapel Hill, Chapel Hill, NC, USA

<sup>2</sup>Tennessee Valley Authority, Muscle Shoals, AL, USA

<sup>3</sup>National Park Service, Gatlinburg, TN USA

<sup>4</sup>School of Engineering and Applied Sciences, Harvard University, Cambridge, MA USA

## Examining the effects of anthropogenic emissions on isoprene-derived SOA formation

S. H. Budisulistiorini et al.

Title Page

Abstract

Introduction

Conclusions

References

Tables

Figures



Back

Close

Full Screen / Esc

Printer-friendly Version

Interactive Discussion



<sup>5</sup>Department of Chemical Engineering, Columbia University, NY, USA

<sup>6</sup>National Exposure Research Laboratory, US Environmental Protection Agency, Research Triangle Park, NC, USA

<sup>7</sup>School of Earth and Atmospheric Sciences, Georgia Institute of Technology, Atlanta, GA, USA

<sup>8</sup>School of Chemical and Biomolecular Engineering, Georgia Institute of Technology, Atlanta, GA, USA

<sup>9</sup>Foundation for Research and Technology, Hellas, Greece

<sup>10</sup>Department of Chemistry, University of Iowa, Iowa City, IA, USA

<sup>11</sup>Department of Experimental Meteorology, Ludwig Maximilian University of Munich, Munich, Germany

<sup>12</sup>Electric Power Research Institute, Palo Alto, CA, USA

\* now at: Battelle, Pueblo, CO, USA

\*\* now at: Ensafe, Nashville, TN, USA

Received: 3 February 2015 – Accepted: 16 February 2015 – Published: 10 March 2015

Correspondence to: J. D. Surratt (surratt@unc.edu)

Published by Copernicus Publications on behalf of the European Geosciences Union.

**Examining the effects of anthropogenic emissions on isoprene-derived SOA formation**

S. H. Budisulistiorini et al.

Title Page

Abstract

Introduction

Conclusions

References

Tables

Figures



Back

Close

Full Screen / Esc

Printer-friendly Version

Interactive Discussion



## Abstract

A suite of offline and real-time gas- and particle-phase measurements was deployed at Look Rock, Tennessee (TN), during the 2013 Southern Oxidant and Aerosol Study (SOAS) to examine the effects of anthropogenic emissions on isoprene-derived secondary organic aerosol (SOA) formation. High- and low-time resolution  $PM_{2.5}$  samples were collected for analysis of known tracer compounds in isoprene-derived SOA by gas chromatography/electron ionization-mass spectrometry (GC/EIMS) and ultra performance liquid chromatography/diode array detection-electrospray ionization-high-resolution quadrupole time-of-flight mass spectrometry (UPLC/DAD-ESI-HR-QTOFMS). Source apportionment of the organic aerosol (OA) was determined by positive matrix factorization (PMF) analysis of mass spectrometric data acquired on an Aerodyne Aerosol Chemical Speciation Monitor (ACSM). Campaign average mass concentrations of the sum of quantified isoprene-derived SOA tracers contributed to ~ 9% (up to 26%) of the total OA mass, with isoprene-epoxydiol (IEPOX) chemistry accounting for ~ 97% of the quantified tracers. PMF analysis resolved a factor with a profile similar to the IEPOX-OA factor resolved in an Atlanta study and was therefore designated IEPOX-OA. This factor was strongly correlated ( $r^2 > 0.7$ ) with 2-methyltetrols,  $C_5$ -alkene triols, IEPOX-derived organosulfates, and dimers of organosulfates, confirming the role of IEPOX chemistry as the source. On average, IEPOX-derived SOA tracer mass was ~ 25% (up to 47%) of the IEPOX-OA factor mass, which accounted for 32% of the total OA. A low-volatility oxygenated organic aerosol (LV-OOA) and an oxidized factor with a profile similar to 91Fac observed in areas where emissions are biogenic-dominated were also resolved by PMF analysis, whereas no primary organic aerosol (POA) sources could be resolved. These findings were consistent with low levels of primary pollutants, such as nitric oxide ( $NO \sim 0.03$  ppb), carbon monoxide ( $CO \sim 116$  ppb), and black carbon ( $BC \sim 0.2 \mu g m^{-3}$ ). Particle-phase sulfate is fairly correlated ( $r^2 \sim 0.3$ ) with both MAE- and IEPOX-derived SOA tracers, and more strongly correlated ( $r^2 \sim 0.6$ ) with the IEPOX-OA factor, in sum suggesting an important role

## Examining the effects of anthropogenic emissions on isoprene-derived SOA formation

S. H. Budisulistiorini et al.

Title Page

Abstract

Introduction

Conclusions

References

Tables

Figures

◀

▶

◀

▶

Back

Close

Full Screen / Esc

Printer-friendly Version

Interactive Discussion













## Examining the effects of anthropogenic emissions on isoprene-derived SOA formation

S. H. Budisulistiorini et al.

Title Page

Abstract

Introduction

Conclusions

References

Tables

Figures

◀

▶

◀

▶

Back

Close

Full Screen / Esc

Printer-friendly Version

Interactive Discussion

site from fresh primary emissions from the valley and allows aged-secondary species to accumulate (Tanner et al., 2005). As described in Tanner et al. (2005), particulate sulfate, black carbon (BC), organic carbon (OC),  $PM_{2.5}$  as well as  $PM_{10}$  and gas-phase sulfur dioxide ( $SO_2$ ), nitric oxide (NO), nitrogen dioxide ( $NO_2$ ), and sum of reactive and reservoir nitrogen oxides ( $NO_y$ ) were measured by a suite of collocated instruments throughout the campaign (Table S1). Meteorological measurements (RH, temperature, wind direction, and wind speed) and  $O_3$  concentrations were acquired at a National Park Service (NPS) shelter across a secondary road opposite the LRK shelter.

### 2.2 ACSM NR- $PM_1$ characterization

Fine ambient aerosol was sampled from the rooftop of the LRK site air-conditioned building during the SOAS campaign. The sampling inlet was approximately 6 m above the ground and equipped with a  $PM_{2.5}$  cyclone. Sample was drawn at  $3 L min^{-1}$  (residence time  $< 2 s$ ) and dried using a nafion drier (PD-200T-24SS, Perma Pure) to maintain RH below 10 % and prevent condensation during sampling. ACSM operation parameters followed those of previous studies (Budisulistiorini et al., 2013, 2014). Briefly, the ACSM scanning rate was set at  $200 ms amu^{-1}$  and data were averaged over 30 min intervals. Data were acquired using ACSM DAQ version 1438 and analyzed using ACSM Local version 1532 (Aerodyne Research, Inc.) within Igor Pro 6.3 (Wavemetrics). Calibrations for sampling flow rate, mass-to-charge ratio ( $m/z$ ), response factor of nitrate ( $RF_{NO_3}$ ), and relative ionization efficiencies of both ammonium ( $RIE_{NH_4}$ ) and sulfate ( $RIE_{SO_4}$ ) were performed three times during the campaign. Mass resolution, heater bias and ionizer voltages, and amplifier zero settings were checked and adjusted daily. A collection efficiency (CE) of 0.5 was applied based on aerosol composition (Middlebrook et al., 2012). Correlations of combined aerosol mass concentrations of ACSM non-refractory (NR)- $PM_1$  and collocated black carbon (BC) with aerosol volume concentrations of  $PM_1$  measured by the Scanning Electrical Mobility System-Mixing Condensation Particle Counter (SEMS-MCPC, Brechtel Manufacturing Inc.) was strong ( $r^2 = 0.89$ ) and suggested an aerosol density of  $1.52 g cm^{-3}$  (Fig. S1),

close to that reported in previous studies in Pasadena, CA (Hayes et al., 2013) and Atlanta, GA (Budisulistiorini et al., 2014). If CE of 1 is used, the estimated aerosol density is  $0.78 \text{ g cm}^{-3}$ , which is much lower than suggested bulk organic and inorganic aerosol densities of  $1.27$  and  $1.77 \text{ g cm}^{-3}$ , respectively (Cross et al., 2007).

## 2.3 OA source characterization

Mass spectra acquired by the ACSM can be represented as a matrix **ORG** where columns  $j$  = observed  $m/z$  values and rows  $i$  = sampling time steps. In a bilinear model, such as PMF, the matrix **ORG** is defined as:

$$\mathbf{ORG}_{i,j} = \sum_{p=1}^P \mathbf{TS}_{i,p} \mathbf{MS}_{p,j} + \mathbf{E}_{i,j} = \widehat{\mathbf{ORG}}_{i,j} + \mathbf{E}_{i,j} \quad (1)$$

where the measured matrix **ORG** is approximated by  $p$  factors with time series (**TS**) and mass spectral profiles (**MS**) of the model solution, and matrix **E** is the difference between the measured matrix and fitted solution. For PMF, (**TS**) and (**MS**) are fitted using a least squares algorithm that minimizes iteratively the quantity  $Q$ , defined as sum of squared residuals weighted by their respective uncertainties:

$$Q = \sum_{i=1}^m \sum_{j=1}^n \left( \frac{e_{ij}}{\sigma_{ij}} \right)^2 \quad (2)$$

When the  $Q$  value is at minimum, all elements in the organic matrix are fit to within their expected error. If the bilinear model is well fitted with minimum errors, the PMF solutions should give  $Q/Q_{\text{exp}}$  close to one.  $Q_{\text{exp}}$  is the expected value of  $Q$  that is approximately equal to number of points of **ORG** ( $t \times m$ ) matrix (Zhang, 2011):

$$Q \approx t \times m \quad (3)$$

Qualitatively, PMF solutions were analysed by running PMF algorithm from different random starting points (Seeds) (Paatero, 2007) and quantitatively by bootstrapping

Title Page

Abstract

Introduction

Conclusions

References

Tables

Figures

◀

▶

◀

▶

Back

Close

Full Screen / Esc

Printer-friendly Version

Interactive Discussion





essary maintenances. July CIMS data was corrected by comparing it to collocated PTR-TOF-MS MVK + MACR data (Sect. 2.4.2) and post-campaign calibration in order to derive a correction factor to account for decay in the micro-channel plate (MCP) detector.

The HR-ToF-CIMS instrument was operated in the negative ion mode using acetate ion chemistry for detection of isoprene-derived epoxides. The acetate ion system efficiently detects small organic acids via deprotonation (Veres et al., 2008; Bertram et al., 2011), such as MAE, and some vicinal diol species, such as the IEPOX, as clusters with the reagent ion. MAE is detected as the  $[\text{C}_4\text{H}_5\text{O}_3]^-$  ion at  $m/z$  101, whereas IEPOX is detected as the  $[\text{CH}_3\text{COO} \cdot \text{C}_5\text{H}_{10}\text{O}_3]^-$  ion at  $m/z$  177 (Fig. S6). IEPOX and its gas-phase precursor, hydroxyhydroperoxides (ISOPOOH), were previously measured by CIMS as cluster ion with  $\text{CF}_3\text{O}^-$  at similar  $m/z$  and were distinguishable through their daughter ions using collision-induced dissociation (Paulot et al., 2009). Recent field and laboratory studies using acetate CIMS found that both ISOPOOH and IEPOX were observed at the same cluster ion at  $m/z$  177, while the deprotonated form at  $m/z$  117 could be attributed solely to IEPOX (D. K. Farmer, personal communication, 2015). In our measurements, interferences of ISOPOOH to the cluster ion  $m/z$  177 could not be differentiated because we could only observe the parent ions unlike Paulot et al. (2009). Moreover, since we operated the acetate ion chemistry HR-ToF-CIMS at different voltage settings than from Farmer et al. (personal communication, 2015), sensitivity of the deprotonated form of IEPOX is very low, and thus it could not be used to quantitatively measure IEPOX and/or to define the fractional contribution of IEPOX and ISOPOOH to the  $m/z$  177 signal. Therefore, we carefully note here that  $m/z$  177 ion measured during this study represents the upper limit of the IEPOX mixing ratio due to ISOPOOH interference at an unknown fraction of the signal.

Gaseous IEPOX and MAE were quantified with HR-ToF-CIMS by applying laboratory-derived calibration factors. All signals were normalized to acetate ion  $[\text{CH}_3\text{COO}]^-$  at  $m/z$  59 to take into account fluctuations in signal arising from changes in pressure during the course of field sampling and calibration. Calibrations were per-

## Examining the effects of anthropogenic emissions on isoprene-derived SOA formation

S. H. Budisulistiorini et al.

Title Page

Abstract

Introduction

Conclusions

References

Tables

Figures

◀

▶

◀

▶

Back

Close

Full Screen / Esc

Printer-friendly Version

Interactive Discussion



cles from the sample flow. The PTR-TOF-MS sub-sampled from this flow at a rate of 0.25 sLpm, resulting in a total inlet transit time of ca. 1–2 s.

PTR-TOF-MS has been described previously by Jordan et al. (2009a, b) and Graus et al. (2010) and was operated in this study as described in Liu et al. (2013).  $\text{H}_3\text{O}^+$  reagent ions were used to selectively ionize organic molecules in the sample air. A high-resolution TOF detector (Tofwerk AG, Switzerland) was used to analyze the reagent and product ions and allowed for exact identification of the ion molecular formula (mass resolution > 4000). The instrument was operated with a drift tube temperature of 80 °C and a drift tube pressure of 2.35 mbar. In  $\text{H}_3\text{O}^+$  mode, the drift tube voltage was set to 520 V, resulting in an E/N of 120 Td (E, electric field strength; N, number density of air in the drift tube; unit, Townsend, Td; 1 Td =  $10^{-17}$  V cm<sup>2</sup>). PTR-TOF-MS spectra were collected at a time resolution of 10 s. Mass calibration was performed every 2 min with data acquisition using the Tof-Daq v1.91 software (Tofwerk AG, Switzerland).

A calibration system was used to establish the instrument sensitivities to VOCs. Gas standards (Scott Specialty Gases) were added into a humidified zero air flow at controlled flow rates. Every 3 h the inlet flow was switched to pass through a catalytic converter (platinum on glass wool heated to 350 °C) to remove VOCs and establish background intensities.

## 2.5 Filter sampling methods and offline chemical analyses

$\text{PM}_{2.5}$  samples were collected on pre-baked Tissuquartz™ Filters (Pall Life Sciences, 8 × 10 in) with three high-volume  $\text{PM}_{2.5}$  samplers (Tisch Environmental, Inc.). All high-volume  $\text{PM}_{2.5}$  samplers were equipped with cyclones operated at  $1 \text{ m}^3 \text{ min}^{-1}$ . One high-volume sampler collected  $\text{PM}_{2.5}$  for 23 h (08:00 to 07:00 the next day, LT), while the two remaining samplers collected  $\text{PM}_{2.5}$  in two cycles. When the sampling schedules were daytime (08:00–19:00, LT) and nighttime (20:00–07:00, LT), the collection cycle and samples are defined as regular day-night sampling periods and samples. On selected days (10–12 June, 14–16 June, 29–30 June, and 9–16 July), when high levels of isoprene, sulfate ( $\text{SO}_4^{2-}$ ), and  $\text{NO}_x$  were predicted at the LRK site by FLEX-

7378

ACPD

15, 7365–7417, 2015

## Examining the effects of anthropogenic emissions on isoprene-derived SOA formation

S. H. Budisulistiorini et al.

Title Page

Abstract

Introduction

Conclusions

References

Tables

Figures

◀

▶

◀

▶

Back

Close

Full Screen / Esc

Printer-friendly Version

Interactive Discussion



## Examining the effects of anthropogenic emissions on isoprene-derived SOA formation

S. H. Budisulistiorini et al.

Title Page

Abstract

Introduction

Conclusions

References

Tables

Figures

◀

▶

◀

▶

Back

Close

Full Screen / Esc

Printer-friendly Version

Interactive Discussion



PART and MOZART model simulations (see SI),  $PM_{2.5}$  were collected more frequently (08:00–11:00, 12:00–15:00, 16:00–19:00, and 20:00–07:00, LT) to capture the effects of anthropogenic pollution on isoprene SOA formation at higher time resolution by offline techniques. Such days are defined as intensive sampling periods and the samples as intensive samples. Forty-seven 23 h integrated and two sets of 64 intensive and 59 day-night filter samples were collected over the six-week period of the campaign and stored at  $-20^{\circ}\text{C}$  until analysis. Field blanks were collected weekly by placing pre-baked quartz filters into the high-volume  $PM_{2.5}$  samplers for 15 min and then removing and storing them under the same conditions as the field samples.

### 2.5.1 Instrumentation

Gas chromatography/electron ionization-mass spectrometry (GC/EI-MS) was performed on a Hewlett-Packard (HP) 5890 Series II Gas Chromatograph equipped with an Econo-Cap<sup>®</sup>-EC<sup>®</sup>-5 Capillary Column (30 m  $\times$  0.25 mm ID; 0.25  $\mu\text{m}$  film thickness) coupled to an HP 5971A Mass Selective Detector. GC/EI-MS operating conditions and temperature program are provided in Surratt et al. (2010).

Ultra performance liquid chromatography/diode array detector-electrospray ionization high-resolution quadrupole time-of-flight mass spectrometry (UPLC/DAD-ESI-HR-QTOFMS) was performed on an Agilent 6500 series system equipped with a Waters Acquity UPLC HSS T3 column (2.1  $\times$  100 mm, 1.8  $\mu\text{m}$  particle size). UPLC/DAD-ESI-HR-QTOFMS operating conditions are described in Zhang et al. (2011).

### 2.5.2 Isoprene-derived SOA tracer quantification

Detailed filter extraction procedures are provided in Lin et al. (2013a). Briefly, from each filter two 37 mm punches (one for analysis by GC/EI-MS and one for UPLC/DAD-ESI-HR-QTOFMS analysis) were extracted in separate pre-cleaned scintillation vials with 20 mL high-purity methanol (LC-MS Chromasolv-grade<sup>®</sup>, Sigma Aldrich) by sonication for 45 min. Filter extracts were then filtered through 0.2  $\mu\text{m}$  syringe filters (Acrodisc<sup>®</sup>





OC/EC analysis using the thermal-optical method (Birch and Cary, 1996) on a Sunset Laboratory (Tigard, OR) OC/EC instrument. Table S4 provides temperature and purge gas settings for the method. The instrument was calibrated internally using methane gas and the calibration was verified with sucrose solution at four mass concentrations.

## 2.6 Estimations of aerosol pH and IEPOX-derived SOA tracers

The thermodynamic model, ISORROPIA-II (Fountoukis and Nenes, 2007; Nenes et al., 1999), is used to estimate aerosol pH. Inputs for the model include aerosol-phase sulfate, nitrate, and ammonium in  $\mu\text{mol m}^{-3}$ , measured by the ACSM under ambient conditions; RH and temperature obtained from National Park Service (NPS); and gas-phase ammonia obtained from Ammonia Monitoring Network (AMoN; TN01/Great Smoky Mountains National Park – Look Rock). ISORROPIA-II predicted particle hydronium ion concentration per volume of air ( $\text{H}^+_{\text{air}}$ ,  $\mu\text{g m}^{-3}$ ), aerosol water (LWC,  $\mu\text{g m}^{-3}$ ), and aerosol aqueous phase mass concentration ( $\mu\text{g m}^{-3}$ ). Aerosol pH is calculated by the following equation:

$$\text{pH} = -\log_{10} a_{\text{H}^+} = -\log_{10} \left( \frac{\text{H}^+_{\text{air}}}{\text{LMASS}} \times \rho_{\text{aer}} \times 1000 \right) \quad (4)$$

where  $a_{\text{H}^+}$  is  $\text{H}^+$  activity in aqueous phase ( $\text{mol L}^{-1}$ ), LMASS is the total liquid-phase aerosol mass ( $\mu\text{g m}^{-3}$ ) and  $\rho_{\text{aer}}$  is aerosol density ( $\text{g cm}^{-3}$ ). The ability of ISORROPIA to capture pH, LWC and gas-to-particle partitioning of inorganic volatiles (e.g.,  $\text{NH}_3$ ,  $\text{HNO}_3$ ,  $\text{HCl}$ ) has been the focus of other studies (Fountoukis et al., 2009; Guo et al., 2014) and is not further discussed here.

IEPOX-derived SOA tracers are estimated using simpleGAMMA (Woo and McNeill, 2015). It is a reduced version of GAMMA (Gas Aerosol Model for Mechanism Analysis), the detailed photochemical box model of aqueous aerosol SOA (aqSOA) formation developed by McNeill and coworkers (McNeill et al., 2012). GAMMA and simpleGAMMA represent aqSOA formation in terms of bulk aqueous uptake followed by aqueous-

## Examining the effects of anthropogenic emissions on isoprene-derived SOA formation

S. H. Budisulistiorini et al.

Title Page

Abstract

Introduction

Conclusions

References

Tables

Figures

◀

▶

◀

▶

Back

Close

Full Screen / Esc

Printer-friendly Version

Interactive Discussion



phase reaction (Schwartz, 1986). For this study, we utilized only the aqueous aerosol-phase chemistry of IEPOX to predict IEPOX-derived SOA constituents. We applied the Henry's law constant of  $3 \times 10^7 \text{ Matm}^{-1}$  for IEPOX partitioning based on measurements by Nguyen et al. (2014) on deliquesced NaCl particles. Estimation of 2-methyltetrols and IEPOX-derived organosulfate masses in the aqueous phase was based on the Eddingsaas et al. (2010) mechanism:



where  $\beta$  is a branching ratio between 2-methyltetrols and IEPOX-derived organosulfate concentration. We applied  $\beta = 0.4$  based on the observation of Eddingsaas et al. (2010) for the most concentrated bulk solution they studied. The rate constant for reaction (5) ( $ka$ ) is a function of  $a_{\text{H}^+}$  and nucleophile concentrations (Eddingsaas et al., 2010), modified to include the possible protonation of IEPOX(aq) by ammonium (Nguyen et al., 2014):

$$ka = k_{\text{H}^+} a_{\text{H}^+} + k_{\text{SO}_4^{2-}} [\text{SO}_4^{2-}] a_{\text{H}^+} + k_{\text{HSO}_4^-} [\text{HSO}_4^-] + k_{\text{NH}_4^+} [\text{NH}_4^+] \quad (6)$$

Here,  $k_{\text{H}^+} = 5 \times 10^{-2} \text{ s}^{-1}$ ,  $k_{\text{SO}_4^{2-}} = 2 \times 10^{-4} \text{ M}^{-1} \text{ s}^{-1}$ , and  $k_{\text{HSO}_4^-} = 7.3 \times 10^{-4} \text{ M}^{-1} \text{ s}^{-1}$ . The ammonium rate constant,  $k_{\text{NH}_4^+}$ , was calculated using GAMMA and the results of the chamber study of Nguyen et al. (2014) to be  $1.7 \times 10^{-5} \text{ M}^{-1} \text{ s}^{-1}$ .

IEPOX uptake and formation of 2-methyltetrols and IEPOX-derived organosulfate was computed using simpleGAMMA with inputs of  $\text{SO}_4^{2-}$ ,  $\text{HSO}_4^-$ ,  $\text{NH}_4^+$ , LWC,  $a_{\text{H}^+}$  concentrations ( $\text{molL}^{-1}$ ), and aerosol pH estimated by ISORROPIA-II simulation of field conditions, ambient temperature and RH, aerosol surface area ( $\text{cm}^2 \text{ cm}^{-3}$ ) obtained from SEMS-MCPC measurements, and IEPOX concentration ( $\text{mol cm}^{-3}$ ) from HR-ToF-CIMS (Sect. 2.4). Masses of SOA tracers formed over 12 h are compared with measurements in Sect. 3.4.2.

## Examining the effects of anthropogenic emissions on isoprene-derived SOA formation

S. H. Budisulistiorini et al.

Title Page

Abstract

Introduction

Conclusions

References

Tables

Figures

◀

▶

◀

▶

Back

Close

Full Screen / Esc

Printer-friendly Version

Interactive Discussion



### 3 Results and discussion

#### 3.1 Fine aerosol component mass concentrations

Chemical measurements of fine aerosol made by the ACSM and collocated instruments are presented in Fig. 1. The ACSM measured a campaign average  $7.6 \pm 4.7 \mu\text{g m}^{-3}$  of NR-PM<sub>1</sub>, which is predominantly organic aerosol (64.1 %). Sulfate aerosol (24.3 %) is the most dominant inorganic aerosol component, followed by ammonium (7.7 %), nitrate (3.8 %), and chloride (0.1 %). The NR-PM<sub>1</sub> mass measured at the site shows strong association ( $r^2 = 0.89$ ) with the SEMS-MCPC PM<sub>1</sub> mass measurements (Figs. 1d and S1).

Moderate correlations, depicted in Fig. S10, were observed between ACSM OM and filter OC and WSOC ( $r^2 = 0.54, 0.39$ , respectively) as well as between filter OC and WSOC measurements ( $r^2 = 0.36$ ), suggesting that fractions of OM and OC at LRK site are water-soluble as previously observed (Turpin and Lim, 2001). This water-soluble fraction may be associated with high isoprene emissions in this area (Zhang et al., 2012a). Lewis et al. (2004) reported that 56–80 % of total carbon in PM<sub>2.5</sub> samples collected during summer in Nashville, TN, was non-fossil carbon, supporting the importance of biogenic SOA in the southeastern US during summer. It is potentially possible that some fraction of this non-fossil carbon is associated to biomass burning (Ke et al., 2007). A more recent study found that non-fossil carbon accounts for 50 % of carbon at two urban sites and 70–100 % of carbon at 10 near-urban or remote sites in the US (Schichtel et al., 2008). In summer 2001, the fraction of non-fossil carbon was reported to vary from 66–80 % of total carbon at the LRK, TN site, suggesting the importance of photochemical oxidation of biogenic VOCs (Tanner et al., 2004). The slope of the linear regression analysis on Fig. S10a indicates an OM : OC ratio of 2.34 and OM : WSOC ratio of 2.19. Using the Aiken et al. (2008) parameterization approach, we found an average ( $\pm 1 - \sigma$ ) OM : OC ratio of 2.14 ( $\pm 0.18$ ). The LRK OM : OC ratios obtained from measurements and parameterization are consistent with a previous study at Look Rock (2.1) (Turpin and Lim, 2001), but higher than that those measured at

Title Page

Abstract

Introduction

Conclusions

References

Tables

Figures

◀

▶

◀

▶

Back

Close

Full Screen / Esc

Printer-friendly Version

Interactive Discussion



Centerville, AL (1.77) (Sun et al., 2011), probably ascribable to different atmospheric aerosol properties at the two sites.

Elemental analyses of ACSM unit-mass resolution data using the Aiken et al. (2008) parameterization results in an average O : C ratio of  $0.77 \pm 0.12$ . This is within 0.6–1 of O : C ratio previously observed in the southeastern US (Centerville, AL). (Sun et al., 2011; Xu et al., 2015).

ACSM sulfate aerosol measurements (average of  $1.85 \pm 1.23 \mu\text{g m}^{-3}$ ) agree well ( $r^2 = 0.67$ , slope 1.08) with the collocated sulfate measurements (Table S1), demonstrating that ACSM performed well when compared to existing air quality monitoring instruments as previously reported (Budisulistiorini et al., 2014). Low nitrate concentration is expected due to the high summer temperatures (15–31 °C) and low prevailing  $\text{NO}_x$  concentrations (0.1–2 ppb) measured at the site. In the absence of a significant source of chloride, chloride concentrations were predictably low ( $0.01 \pm 0.01 \mu\text{g m}^{-3}$ ).

On average, mass concentration of BC was  $0.23 \pm 0.14 \mu\text{g m}^{-3}$  or about 3% of total  $\text{PM}_{2.5}$  measured at the site. The low relative contribution was consistent during the campaign except on 11 to 12 July when there was a significant increase during few hours overnight. EC measured from filters was even lower at  $0.06 \mu\text{g m}^{-3}$  on average and was only weakly correlated ( $r^2 = 0.32$ ) with BC. Carbon monoxide (CO), another primary species measured at LRK, was also low ( $115.62 \pm 24.06$  ppb on average) throughout the campaign. A previous study found that the level of primary species increased during mid-morning when the boundary layer height reached the site, and declined later in the day as a result of dilution (Tanner et al., 2005). In contrast, secondary species such as  $\text{PM}_{2.5}$  and sulfate do not show significant diurnal variability, suggesting local meteorological conditions are less influential in determining concentrations of the long-lived species (Tanner et al., 2005). The overall low concentration of primary emissions at the site (Fig. S11) is consistent with minimum local and/or regional primary emissions.

**Examining the effects of anthropogenic emissions on isoprene-derived SOA formation**

S. H. Budisulistiorini et al.

Title Page

Abstract

Introduction

Conclusions

References

Tables

Figures

◀

▶

◀

▶

Back

Close

Full Screen / Esc

Printer-friendly Version

Interactive Discussion



### 3.2 Source apportionment of OA from the ACSM

PMF analysis was conducted on the ACSM OA mass spectral data in order to resolve factors (or source profiles) without a-priori assumptions. A 3 factor solution resolved from PMF analysis, as shown in Figs. 2 and 3, was selected as the best-fit (see SI for details of  $Q/Q_{\text{exp}}$ ,  $f_{\text{peak}}$ , etc.), comprised of the known LV-OOA factor (Jimenez et al., 2009; Ulbrich et al., 2009), an IEPOX-OA factor (Budisulistiorini et al., 2013; Slowik et al., 2011; Robinson et al., 2011), and a factor similar to 91Fac, a factor previously observed in areas dominated by biogenic emissions (Robinson et al., 2011; Slowik et al., 2011; Chen et al., 2014).

The IEPOX-OA factor resolved from our dataset is more closely correlated to sulfate measured by the ACSM ( $r^2 = 0.58$ ) than by the collocated instrument ( $r^2 = 0.31$ ) (Table S5). Correlation of gaseous IEPOX measured by HR-ToF-CIMS with the IEPOX-OA factor is low ( $r^2 = 0.24$ ), which may be a consequence of IEPOX uptake onto sulfate aerosol upwind of the sampling site, since IEPOX has an estimated lifetime of 5 h in the presence of aqueous, highly acidic aerosol ( $\text{pH} \leq 1$ ) (Gaston et al., 2014). Importantly, the IEPOX-OA factor correlates strongly with 2-methyltetrols ( $r^2 = 0.80$ ), IEPOX-derived organosulfate ( $r^2 = 0.81$ ),  $\text{C}_5$ -alkene triols ( $r^2 = 0.75$ ), and dimers of organosulfate ( $r^2 = 0.73$ ) (Table 2), giving an overall  $r^2$  of 0.83 with sum of IEPOX-derived SOA tracers measured by offline techniques. The high correlation provides strong evidence that IEPOX chemistry gives rise to the PMF factor we have designated as the IEPOX-OA factor. The contribution of this factor to total OM is 32 %, which is strikingly consistent with the contribution of the factor designated as the IEPOX-OA factor in the PMF analysis of fine organic aerosol collected in downtown Atlanta, GA (Budisulistiorini et al., 2013) and across other sites in this region (Xu et al., 2015). Located on a ridge top above the morning valley fog, LRK receives air masses from the valley as the boundary layer rises during the day (Tanner et al., 2005). As a consequence, IEPOX-derived SOA from surrounding forested and isoprene-rich areas were likely continuously oxidized during transport to the sampling site. Transport from dis-

## Examining the effects of anthropogenic emissions on isoprene-derived SOA formation

S. H. Budisulistiorini et al.

Title Page

Abstract

Introduction

Conclusions

References

Tables

Figures

◀

▶

◀

▶

Back

Close

Full Screen / Esc

Printer-friendly Version

Interactive Discussion



## Examining the effects of anthropogenic emissions on isoprene-derived SOA formation

S. H. Budisulistorini et al.

Title Page

Abstract

Introduction

Conclusions

References

Tables

Figures

◀

▶

◀

▶

Back

Close

Full Screen / Esc

Printer-friendly Version

Interactive Discussion

5 tant origins may also explain the lack of significant diurnal variation (Fig. 3) of the IEPOX-OA factor at LRK in contrast to the behavior of the IEPOX-OA factor observed in Atlanta (Budisulistorini et al., 2013). Despite the strong diurnal profile of isoprene at LRK site, diurnal variations of the gas-phase products of isoprene photooxidation (i.e., MVK + MACR, IEPOX and MAE) were small during this campaign (Fig. 4). The small diurnal variation of IEPOX might explain the small diurnal variation of the IEPOX-OA factor. WSOC shows fair correlation with some IEPOX-OA tracers ( $r^2 = 0.3$ – $0.4$ ; Table S6) and IEPOX-OA factor ( $r^2 = 0.37$ ; Table S5) the nature of which will be discussed in more detail below.

10 The LV-OOA factor contributes 50 % of OM (Fig. 3). The average  $f_{44} = 0.22$  is comparable to that of the standard LV-OOA profile (Ng et al., 2011), suggesting it is an oxidized (aged) aerosol. The LV-OOA correlated well with nitrate ( $r^2 = 0.62$ ) but more weakly with sulfate ( $r^2 = 0.39$ ) (Table S5). Correlation with nitrate as well as the high level of oxidation is consistent with the suggestion above that a fraction of OA originates in the valley. In the valley, OA formation would be influenced by nitrate chemistry or anthropogenic emissions and age during transport to the LRK site.

15 The 91Fac factor is characterized by a distinct ion at  $m/z$  91. At LRK, the average  $f_{44}$  of 91Fac is 0.12, between the values 0.05 and 0.16 reported for standard SV-OOA and LV-OOA profiles, respectively (Ng et al., 2011), indicating that it is likely an oxygenated OA. The LRK 91Fac makes the smallest contribution to OM (18 %) of the three factors resolved by PMF analysis. The 91Fac diurnal pattern shows slight increases during noon and night, suggesting that this factor might be affected by both photochemistry and nighttime chemistry. The source of 91Fac is currently a matter of speculation. Aged biomass burning aerosol (Robinson et al., 2011) has been suggested because of the similarity of the profile to that of biomass burning aerosols, except for absence of prominent ions at  $m/z$  60 and 73 expected from levoglucosan (Alfarra et al., 2007). A more recent study proposed that fresh BVOC (i.e., monoterpene) oxidation products are a possible source based on chamber experiments (Chen et al., 2014). At LRK, 91Fac correlates moderately well with a monoterpene-derived organosulfate



derived SOA tracers compared to MAE-derived tracers. It should be noted that IEPOX quantified here includes the interference of ISOPOOH on its signal; however, the overall measured IEPOX signal is still substantially higher than the MAE signal, even if we assume IEPOX only contributes to 1–10% of the  $m/z$  177 intensity.

In sum, IEPOX- and MAE-derived tracers contributed 96.8 and 8.8%, respectively, of total isoprene-derived SOA mass. This observation is consistent with a previous field study in Yorkville, GA, which reported the summed IEPOX-derived SOA tracers comprised 97.5% of the quantified isoprene-derived SOA mass (Lin et al., 2013a). Total IEPOX-derived tracers masses were on average 24.6% (maximum 46.8%) of the IEPOX-OA factor mass. This is consistent with a recent laboratory study of isoprene photooxidation under high HO<sub>2</sub> conditions that suggested IEPOX isomers contributed about 50% of SOA mass formed (Liu et al., 2014).

Masses of IEPOX- and MAE-derived SOA tracers were fairly correlated ( $r^2 = 0.36$  and 0.29, respectively) with WSOC (Fig. S10c). Around 24% of the WSOC mass might be explained by IEPOX-derived SOA tracer masses, which consist predominantly of 2-methyltetrols, C<sub>5</sub>-alkene triols, and IEPOX-derived organosulfates. The tetrols and triols are hydrophilic compounds owing to the OH groups, and the organosulfates are ionic polar compounds (Gómez-González et al., 2008).

An interesting and potentially important observation is that oligomeric IEPOX-derived humic-like substances (HULIS) have been reported in both reactive uptake experiments onto acidified sulfate seed aerosol and ambient fine aerosol (Lin et al., 2014). The HULIS is a mixture of hydroxylated, sulfated as well as highly unsaturated, light-absorbing components which may partition between WSOC and water insoluble organic carbon (WISC) fractions (Lin et al., 2014). This finding might also in part explain the moderate correlation between WSOC and the IEPOX-OA factor. However, HULIS has not been quantified here due to the lack of authentic standards, but will likely help to close the IEPOX-OA mass budget once appropriate standards are developed and applied. As quantified by ACSM, summed isoprene-derived SOA tracers on average accounted for 0.5 μg m<sup>-3</sup> or 9.1% (up to 4.1 μg m<sup>-3</sup> or 26.4%) of the average organic

## Examining the effects of anthropogenic emissions on isoprene-derived SOA formation

S. H. Budisulistiorini et al.

[Title Page](#)[Abstract](#)[Introduction](#)[Conclusions](#)[References](#)[Tables](#)[Figures](#)[◀](#)[▶](#)[◀](#)[▶](#)[Back](#)[Close](#)[Full Screen / Esc](#)[Printer-friendly Version](#)[Interactive Discussion](#)







## Examining the effects of anthropogenic emissions on isoprene-derived SOA formation

S. H. Budisulistiorini et al.

Title Page

Abstract

Introduction

Conclusions

References

Tables

Figures

◀

▶

◀

▶

Back

Close

Full Screen / Esc

Printer-friendly Version

Interactive Discussion

of Pye et al. (2013), the model underestimated the 2-methyltetrols and IEPOX-derived organosulfates by 31 and 1 %, respectively. Decreasing the  $H^*$  by one order of magnitude yielded a factor of  $\sim 10$  decrease in the in predicted IEPOX SOA tracers mass, which is consistent with Pye et al. (2013) observation in sensitivity studies that a factor of 7 increase in  $H^*$  yielded a factor of  $\sim 5$  increase in predicted IEPOX SOA yield. Similarly, summed masses of the modeled SOA tracers (Fig. 7) yielded a 115 % ( $r^2 = 0.57$ ) overestimate of the IEPOX-OA factor, whereas summed SOA tracers modeled by assuming  $H^*$  of one order of magnitude lower yielded an 83 % underestimate of the IEPOX-OA factor ( $r^2 = 0.56$ ). simpleGAMMA predicts only subset of IEPOX-derived SOA tracers, thus underestimation of the predicted tracers to IEPOX-OA factor is expected.

In addition to the uncertainty in the  $H^*$  parameter, several other factors may also contribute to mass disagreement between the tracer estimated by simpleGAMMA and the field data. The box model simulations took locally measured IEPOX and aerosol parameters as inputs, and simulated 12 h of reactive processing, rather than simulating uptake, reaction, and transport along a trajectory initiating in the valley. The locally measured IEPOX signal is noted above to have interference from ISOPOOH, thus the model outputs likely overestimate the measurements. Additionally,  $C_5$ -alkene triols, the third largest contributor to the IEPOX-derived SOA tracers, and oligomeric HULIS are not included in the simpleGAMMA model estimation. Neglect of the  $C_5$ -alkene triols and oligomers as well as yet unknown IEPOX-derived SOA formation pathways by this model could contribute to inaccuracy in estimation of the mass contribution of 2-methyltetrols and IEPOX-derived organosulfates to the total amount of IEPOX-derived SOA tracers and reduce the correlation. Finally, oxidative aging of IEPOX SOA tracers is not included in simpleGAMMA at this time due to current lack of availability of kinetic and mechanistic data. Overall, although mass disagreement persists, good correlation between model and field measurements of tracers suggest that the uptake mechanism of IEPOX is consistent with acid-catalyzed mechanism proposed from ki-

netic (Eddingsaas et al., 2010; Pye et al., 2013) and laboratory studies (Lin et al., 2012; Nguyen et al., 2014).

## 4 Conclusions

Offline chemical analysis of PM<sub>2.5</sub> samples collected from LRK, TN, during the 2013 SOAS campaign show a substantial contribution by IEPOX-derived SOA tracers to the total OA mass (~ 9% on average, up to 26%). A larger contribution (32%) to total OA mass is estimated by PMF analysis of the real-time ACSM OA mass spectrometric data. Overall, the importance of IEPOX heterogeneous chemistry in this region is clearly demonstrable. No association was observed between the gas-phase constituents NO and NO<sub>2</sub> and the IEPOX-derived SOA tracers or the IEPOX-OA factor suggesting that IEPOX-derived SOA formed upwind or distant from the sampling site. Moderate association between NO<sub>y</sub> and MAE-/HMML-derived SOA tracers was observed, consistent with the proposed involvement of oxidizing nitrogen compounds in MAE-/HMML-derived SOA formation (Lin et al., 2013b; Nguyen et al., 2015). Particle-phase sulfate is fairly correlated ( $r^2 = 0.3\text{--}0.4$ ) with both MAE-/HMML- and IEPOX-derived SOA tracers, and more strongly correlated ( $r^2 \sim 0.6$ ) with the IEPOX-OA factor, overall suggesting that sulfate plays an important role in isoprene SOA formation. However, this association requires further analysis, in light of the proposed formation of IEPOX-derived SOA during transport to LRK from an upwind or down-slope origin. Several explanations may be proposed for the lack of a strong association between isoprene-derived SOA mass and particle acidity: (1) isoprene-derived SOA is not strongly limited by levels of predicted aerosol acidity and LWC even though these are in the favored ranges (pH < 2) to promote sufficient SOA production based on recent laboratory kinetic studies (Gaston et al., 2014; Riedel et al., 2015) and thus, other potentially unknown controlling factors in this region might need to be considered; (2) no strong correlation exists between SOA mass and local aerosol acidity which estimation is challenging due to changes in particle composition and characteristics during reac-

## Examining the effects of anthropogenic emissions on isoprene-derived SOA formation

S. H. Budisulistiorini et al.

Title Page

Abstract

Introduction

Conclusions

References

Tables

Figures



Back

Close

Full Screen / Esc

Printer-friendly Version

Interactive Discussion



tive uptake and (3) several key inter-related variables (LWC, aerosol surface area and aerosol acidity) control SOA yield and thus the correlation of aerosol acidity and SOA yield will be difficult to deconvolute from complex field data until modeling can better constrain these effects. Consistent with the suggestion that IEPOX-derived SOA forms during transport from distant locations, air mass back-trajectory indicated that westerly flow from potential sources of oxidation products where biogenic and anthropogenic emissions can mix, are likely related to episodes of high levels of IEPOX-derived SOA measured at LRK. In contrast, when air masses originated mainly from forested and rural areas to the south and southeast of the site, high levels of IEPOX-derived SOA mass were not observed. Good correlation between SOA model outputs and field measurements suggests that gaps remain in our knowledge of isoprene-derived SOA formation. Laboratory studies are needed to reduce the uncertainty in the effective Henry's Law constant,  $H^*$ , for IEPOX. Additional studies are needed to further quantify the condensed-phase mechanism and kinetics of SOA formation via the IEPOX pathway so that it may be represented in more detail in models. Notwithstanding, initial modeling results allow critical insight into how more explicit treatment of the reactions between anthropogenic pollutants and isoprene oxidation products may be incorporated into models of SOA formation. Importantly, by inclusion of explicit IEPOX- and MAE-derived SOA formation pathways in a model, Pye et al. (2013) recently demonstrated that by lowering  $\text{SO}_x$  emissions in the eastern US by 25 % could lower IEPOX- and MAE-derived SOA formation 35 to 40 %. Future studies should attempt to improve model predictions of IEPOX-derived SOA formation and systematically examine effects of implementing stricter  $\text{SO}_x$  controls in this region.

**The Supplement related to this article is available online at  
doi:10.5194/acpd-15-7365-2015-supplement.**

*Acknowledgements.* This work was funded by the U.S. Environmental Protection Agency (EPA) through grant number 835404. The contents of this publication are solely the responsibility of

## Examining the effects of anthropogenic emissions on isoprene-derived SOA formation

S. H. Budisulistiorini et al.

Title Page

Abstract

Introduction

Conclusions

References

Tables

Figures

◀

▶

◀

▶

Back

Close

Full Screen / Esc

Printer-friendly Version

Interactive Discussion



## Examining the effects of anthropogenic emissions on isoprene-derived SOA formation

S. H. Budisulistiorini et al.

Title Page

Abstract

Introduction

Conclusions

References

Tables

Figures

◀

▶

◀

▶

Back

Close

Full Screen / Esc

Printer-friendly Version

Interactive Discussion



the authors and do not necessarily represent the official views of the U.S. EPA. Further, the U.S. EPA does not endorse the purchase of any commercial products or services mentioned in the publication. The U.S. EPA through its Office of Research and Development collaborated in the research described here. It has been subjected to Agency review and approved for publication, but may not necessarily reflect official Agency policy. The author would also like to thank the Electric Power Research Institute (EPRI) for their support. This study was supported in part by the National Oceanic and Atmospheric Administration (NOAA) Climate Program Office's AC4 program, award #NA13OAR4310064. We thank Bill Hicks of the Tennessee Valley Authority (TVA) for his assistance in collecting the collocated monitoring data at the LRK site. S. H. Budisulistiorini was supported by a Fulbright Presidential Fellowship (2010–2013) for attending the University of North Carolina at Chapel Hill and the UNC Graduate School Off-Campus Dissertation Research Fellowship, as well as partial appointment to the Internship/Research Participation Program at the Office of Research and Development, U.S. EPA, administered by the Oak Ridge Institute for Science and Education through an interagency agreement between the U.S. Department of Energy and EPA. M. Neff and E. A. Stone were supported by US EPA Science to Achieve Results (STAR) program grant number 835401. The authors thank Lynn Russell, Timothy Bertram and Christopher Cappa as well as their respective groups for their collaboration during the SOAS campaign at LRK. The authors thank Louisa Emmons for her assistance with forecasts made available during the SOAS campaign. The authors thank John Offenberg for providing access to Sunset OC/EC analysis instrument. The authors also thank Tianqu Cui for his assistance in helping deploy instrumentation from the UNC group, and Wendy Marth and Theran Riedel for their assistance in helping calibrate the HR-ToF-CIMS. We would like to thank Annmarie Carlton, Joost deGouw, Jose Jimenez, and Allen Goldstein for helping to organize the SOAS campaign and coordinating communication between ground sites.

## References

Aiken, A. C., DeCarlo, P. F., Kroll, J. H., Worsnop, D. R., Huffman, J. A., Docherty, K. S., Ulbrich, I. M., Mohr, C., Kimmel, J. R., Sueper, D., Sun, Y., Zhang, Q., Trimborn, A., Northway, M., Ziemann, P. J., Canagaratna, M. R., Onasch, T. B., Alfarra, M. R., Prevot, A. S. H., Dommen, J., Duplissy, J., Metzger, A., Baltensperger, U., and Jimenez, J. L.: O/C and OM/OC ratios of primary, secondary, and ambient organic aerosols with high-

## Examining the effects of anthropogenic emissions on isoprene-derived SOA formation

S. H. Budisulistiorini et al.

Title Page

Abstract

Introduction

Conclusions

References

Tables

Figures

◀

▶

◀

▶

Back

Close

Full Screen / Esc

Printer-friendly Version

Interactive Discussion

resolution time-of-flight aerosol mass spectrometry, *Environ. Sci. Technol.*, 42, 4478–4485, doi:10.1021/es703009q, 2008.

Alfarra, M. R., Prevot, A. S. H., Szidat, S., Sandradewi, J., Weimer, S., Lanz, V. A., Schreiber, D., Mohr, M., and Baltensperger, U.: Identification of the mass spectral signature of organic aerosols from wood burning emissions, *Environ. Sci. Technol.*, 41, 5770–5777, doi:10.1021/es062289b, 2007.

Bates, K. H., Crounse, J. D., St. Clair, J. M., Bennett, N. B., Nguyen, T. B., Seinfeld, J. H., Stoltz, B. M., and Wennberg, P. O.: Gas phase production and loss of isoprene epoxydiols, *J. Phys. Chem. A*, 118, 1237–1246, doi:10.1021/jp4107958, 2014.

Bertram, T. H., Kimmel, J. R., Crisp, T. A., Ryder, O. S., Yatavelli, R. L. N., Thornton, J. A., Cubison, M. J., Gonin, M., and Worsnop, D. R.: A field-deployable, chemical ionization time-of-flight mass spectrometer, *Atmos. Meas. Tech.*, 4, 1471–1479, doi:10.5194/amt-4-1471-2011, 2011.

Birch, M. E. and Cary, R. A.: Elemental carbon-based method for occupational monitoring of particulate diesel exhaust: methodology and exposure issues, *Analyst*, 121, 1183–1190, doi:10.1039/AN9962101183, 1996.

Budisulistiorini, S. H., Canagaratna, M. R., Croteau, P. L., Marth, W. J., Baumann, K., Edgerton, E. S., Shaw, S. L., Knipping, E. M., Worsnop, D. R., Jayne, J. T., Gold, A., and Surratt, J. D.: Real-time continuous characterization of secondary organic aerosol derived from isoprene epoxydiols in downtown Atlanta, Georgia, using the aerodyne aerosol chemical speciation monitor, *Environ. Sci. Technol.*, 47, 5686–5694, doi:10.1021/es400023n, 2013.

Budisulistiorini, S. H., Canagaratna, M. R., Croteau, P. L., Baumann, K., Edgerton, E. S., Kollman, M. S., Ng, N. L., Verma, V., Shaw, S. L., Knipping, E. M., Worsnop, D. R., Jayne, J. T., Weber, R. J., and Surratt, J. D.: Intercomparison of an Aerosol Chemical Speciation Monitor (ACSM) with ambient fine aerosol measurements in downtown Atlanta, Georgia, *Atmos. Meas. Tech.*, 7, 1929–1941, doi:10.5194/amt-7-1929-2014, 2014.

Carlton, A. G., Bhawe, P. V., Napelenok, S. L., Edney, E. O., Sarwar, G., Pinder, R. W., Pouliot, G. A., and Houyoux, M.: Model representation of secondary organic aerosol in CMAQv4.7, *Environ. Sci. Technol.*, 44, 8553–8560, doi:10.1021/es100636q, 2010.

Chan, M. N., Surratt, J. D., Claeys, M., Edgerton, E. S., Tanner, R. L., Shaw, S. L., Zheng, M., Knipping, E. M., Eddingsaas, N. C., Wennberg, P. O., and Seinfeld, J. H.: Characterization and quantification of isoprene-derived epoxydiols in ambient aerosol in the southeastern United States, *Environ. Sci. Technol.*, 44, 4590–4596, doi:10.1021/es100596b, 2010.

---

**Examining the effects  
of anthropogenic  
emissions on  
isoprene-derived  
SOA formation**

---

S. H. Budisulistiorini et al.

---

[Title Page](#)[Abstract](#)[Introduction](#)[Conclusions](#)[References](#)[Tables](#)[Figures](#)[◀](#)[▶](#)[◀](#)[▶](#)[Back](#)[Close](#)[Full Screen / Esc](#)[Printer-friendly Version](#)[Interactive Discussion](#)

Chen, Q., Farmer, D. K., Rizzo, L. V., Pauliquevis, T., Kuwata, M., Karl, T. G., Guenther, A., Allan, J. D., Coe, H., Andreae, M. O., Pöschl, U., Jimenez, J. L., Artaxo, P., and Martin, S. T.: Fine-mode organic mass concentrations and sources in the Amazonian wet season (AMAZE-08), *Atmos. Chem. Phys. Discuss.*, 14, 16151–16186, doi:10.5194/acpd-14-16151-2014, 2014.

5 Claeys, M., Graham, B., Vas, G., Wang, W., Vermeylen, R., Pashynska, V., Cafmeyer, J., Guyon, P., Andreae, M. O., Artaxo, P., and Maenhaut, W.: Formation of secondary organic aerosols through photooxidation of isoprene, *Science*, 303, 1173–1176, doi:10.1126/science.1092805, 2004.

10 Cross, E. S., Slowik, J. G., Davidovits, P., Allan, J. D., Worsnop, D. R., Jayne, J. T., Lewis, D. K., Canagaratna, M., and Onasch, T. B.: Laboratory and ambient particle density determinations using light scattering in conjunction with aerosol mass spectrometry, *Aerosol Sci. Tech.*, 41, 343–359, doi:10.1080/02786820701199736, 2007.

15 Ding, X., Wang, X., Gao, B., Fu, X., He, Q., Zhao, X., Yu, J., and Zheng, M.: Tracer-based estimation of secondary organic carbon in the Pearl River Delta, south China, *J. Geophys. Res.*, 117, D05313, doi:10.1029/2011JD016596, 2012.

Dockery, D. W., Pope, C. A., Xu, X., Spengler, J. D., Ware, J. H., Fay, M. E., Ferris, B. G., and Speizer, F. E.: An association between air pollution and mortality in six U. S. cities, *New Engl. J. Med.*, 329, 1753–1759, doi:10.1056/NEJM199312093292401, 1993.

20 Eddingsaas, N. C., VanderVelde, D. G., and Wennberg, P. O.: Kinetics and products of the acid-catalyzed ring-opening of atmospherically relevant butyl epoxy alcohols, *J. Phys. Chem. A*, 114, 8106–8113, doi:10.1021/jp103907c, 2010.

25 Edney, E. O., Kleindienst, T. E., Jaoui, M., Lewandowski, M., Offenberg, J. H., Wang, W., and Claeys, M.: Formation of 2-methyl tetrols and 2-methylglyceric acid in secondary organic aerosol from laboratory irradiated isoprene/NO<sub>x</sub>/SO<sub>2</sub>/air mixtures and their detection in ambient PM<sub>2.5</sub> samples collected in the eastern United States, *Atmos. Environ.*, 39, 5281–5289, doi:10.1016/j.atmosenv.2005.05.031, 2005.

30 Foley, K. M., Roselle, S. J., Appel, K. W., Bhave, P. V., Pleim, J. E., Otte, T. L., Mathur, R., Sarwar, G., Young, J. O., Gilliam, R. C., Nolte, C. G., Kelly, J. T., Gilliland, A. B., and Bash, J. O.: Incremental testing of the Community Multiscale Air Quality (CMAQ) modeling system version 4.7, *Geosci. Model Dev.*, 3, 205–226, doi:10.5194/gmd-3-205-2010, 2010.



---

**Examining the effects  
of anthropogenic  
emissions on  
isoprene-derived  
SOA formation**S. H. Budisulistiorini et al.

---

[Title Page](#)[Abstract](#)[Introduction](#)[Conclusions](#)[References](#)[Tables](#)[Figures](#)[◀](#)[▶](#)[◀](#)[▶](#)[Back](#)[Close](#)[Full Screen / Esc](#)[Printer-friendly Version](#)[Interactive Discussion](#)

mann, T., Iinuma, Y., Jang, M., Jenkin, M. E., Jimenez, J. L., Kiendler-Scharr, A., Maenhaut, W., McFiggans, G., Mentel, Th. F., Monod, A., Prévôt, A. S. H., Seinfeld, J. H., Surratt, J. D., Szmigielski, R., and Wildt, J.: The formation, properties and impact of secondary organic aerosol: current and emerging issues, *Atmos. Chem. Phys.*, 9, 5155–5236, doi:10.5194/acp-9-5155-2009, 2009.

Hayes, P. L., Ortega, A. M., Cubison, M. J., Froyd, K. D., Zhao, Y., Cliff, S. S., Hu, W. W., Toohey, D. W., Flynn, J. H., Lefer, B. L., Grossberg, N., Alvarez, S., Rappenglück, B., Taylor, J. W., Allan, J. D., Holloway, J. S., Gilman, J. B., Kuster, W. C., de Gouw, J. A., Massoli, P., Zhang, X., Liu, J., Weber, R. J., Corrigan, A. L., Russell, L. M., Isaacman, G., Worton, D. R., Kreisberg, N. M., Goldstein, A. H., Thalman, R., Waxman, E. M., Volkamer, R., Lin, Y. H., Surratt, J. D., Kleindienst, T. E., Offenberg, J. H., Dusanter, S., Griffith, S., Stevens, P. S., Brioude, J., Angevine, W. M., and Jimenez, J. L.: Organic aerosol composition and sources in Pasadena, California during the 2010 CalNex campaign, *J. Geophys. Res.*, 118, 9233–9233, doi:10.1002/jgrd.50530, 2013.

Hsu, S. O. -I., Ito, K., and Lippmann, M.: Effects of thoracic and fine PM and their components on heart rate and pulmonary function in COPD patients, *J. Expo. Sci. Env. Epid.*, 21, 464–472, 2011.

IPCC: Climate change 2013: The physical science basis, in: Fifth Assessment Report to the Intergovernmental Panel on Climate Change, contribution of working group I, Cambridge University Press, Cambridge, UK and New York, NY, USA, 2013.

Jacobs, M. I., Darer, A. I., and Elrod, M. J.: Rate constants and products of the OH reaction with isoprene-derived epoxides, *Environ. Sci. Technol.*, 47, 12868–12876, doi:10.1021/es403340g, 2013.

Jang, M., Czoschke, N. M., Lee, S., and Kamens, R. M.: Heterogeneous atmospheric aerosol production by acid-catalyzed particle-phase reactions, *Science*, 298, 814–817, doi:10.1126/science.1075798, 2002.

Jimenez, J. L., Canagaratna, M. R., Donahue, N. M., Prevot, A. S. H., Zhang, Q., Kroll, J. H., DeCarlo, P. F., Allan, J. D., Coe, H., Ng, N. L., Aiken, A. C., Docherty, K. S., Ulbrich, I. M., Grieshop, A. P., Robinson, A. L., Duplissy, J., Smith, J. D., Wilson, K. R., Lanz, V. A., Hueglin, C., Sun, Y. L., Tian, J., Laaksonen, A., Raatikainen, T., Rautiainen, J., Vaattovaara, P., Ehn, M., Kulmala, M., Tomlinson, J. M., Collins, D. R., Cubison, M. J., E., Dunlea, J., Huffman, J. A., Onasch, T. B., Alfarra, M. R., Williams, P. I., Bower, K., Kondo, Y., Schneider, J., Drewnick, F., Borrmann, S., Weimer, S., Demerjian, K., Salcedo, D., Cot-

**Examining the effects  
of anthropogenic  
emissions on  
isoprene-derived  
SOA formation**

S. H. Budisulistiorini et al.

Title Page

Abstract

Introduction

Conclusions

References

Tables

Figures

◀

▶

◀

▶

Back

Close

Full Screen / Esc

Printer-friendly Version

Interactive Discussion

trell, L., Griffin, R., Takami, A., Miyoshi, T., Hatakeyama, S., Shimono, A., Sun, J. Y., Zhang, Y. M., Dzepina, K., Kimmel, J. R., Sueper, D., Jayne, J. T., Herndon, S. C., Trimborn, A. M., Williams, L. R., Wood, E. C., Middlebrook, A. M., Kolb, C. E., Baltensperger, U., and Worsnop, D. R.: Evolution of organic aerosols in the atmosphere, *Science*, 326, 1525–1529, doi:10.1126/science.1180353, 2009.

Jordan, A., Haidacher, S., Hanel, G., Hartungen, E., Herbig, J., Märk, L., Schottkowsky, R., Seehauser, H., Sulzer, P., and Märk, T. D.: An online ultra-high sensitivity proton-transfer-reaction mass-spectrometer combined with switchable reagent ion capability (PTR + SRI – MS), *Int. J. Mass. Spectrom.*, 286, 32–38, doi:10.1016/j.ijms.2009.06.006, 2009a.

Jordan, A., Haidacher, S., Hanel, G., Hartungen, E., Märk, L., Seehauser, H., Schottkowsky, R., Sulzer, P., and Märk, T. D.: A high resolution and high sensitivity proton-transfer-reaction time-of-flight mass spectrometer (PTR-TOF-MS), *Int. J. Mass. Spectrom.*, 286, 122–128, doi:10.1016/j.ijms.2009.07.005, 2009b.

Kalberer, M., Paulsen, D., Sax, M., Steinbacher, M., Dommen, J., Prevot, A. S. H., Fisseha, R., Weingartner, E., Frankevich, V., Zenobi, R., and Baltensperger, U.: Identification of polymers as major components of atmospheric organic aerosols, *Science*, 303, 1659–1662, 2004.

Kamens, R. M., Gery, M. W., Jeffries, H. E., Jackson, M., and Cole, E. I.: Ozone? isoprene reactions: product formation and aerosol potential, *Int. J. Chem. Kinet.*, 14, 955–975, doi:10.1002/kin.550140902, 1982.

Karambelas, A., Pye, H. O. T., Budisulistiorini, S. H., Surratt, J. D., and Pinder, R. W.: Contribution of isoprene epoxydiol to urban organic aerosol: evidence from modeling and measurements, *Environ. Sci. Technol. Lett.*, 1, 278–283, doi:10.1021/ez5001353, 2014.

Ke, L., Ding, X., Tanner, R. L., Schauer, J. J., and Zheng, M.: Source contributions to carbonaceous aerosols in the Tennessee Valley region, *Atmos. Environ.*, 41, 8898–8923, doi:10.1016/j.atmosenv.2007.08.024, 2007.

Kourtchev, I., Copolovici, L., Claeys, M., and Maenhaut, W.: Characterization of atmospheric aerosols at a forested site in Central Europe, *Environ. Sci. Technol.*, 43, 4665–4671, doi:10.1021/es803055w, 2009.

Kroll, J. H., Ng, N. L., Murphy, S. M., Flagan, R. C., and Seinfeld, J. H.: Secondary organic aerosol formation from isoprene photooxidation, *Environ. Sci. Technol.*, 40, 1869–1877, 2006.

---

**Examining the effects  
of anthropogenic  
emissions on  
isoprene-derived  
SOA formation**

---

S. H. Budisulistorini et al.

---

[Title Page](#)[Abstract](#)[Introduction](#)[Conclusions](#)[References](#)[Tables](#)[Figures](#)[◀](#)[▶](#)[◀](#)[▶](#)[Back](#)[Close](#)[Full Screen / Esc](#)[Printer-friendly Version](#)[Interactive Discussion](#)

Lewis, C. W., Klouda, G. A., and Ellenson, W. D.: Radiocarbon measurement of the biogenic contribution to summertime PM-2.5 ambient aerosol in Nashville, TN, *Atmos. Environ.*, **38**, 6053–6061, doi:10.1016/j.atmosenv.2004.06.011, 2004.

Lin, Y., Zhang, Z., Docherty, K. S., Zhang, H., Budisulistorini, S. H., Rubitschun, C. L., Shaw, S. L., Knipping, E. M., Edgerton, E. S., Kleindienst, T. E., Gold, A., and Surratt, J. D.: Isoprene epoxydiols as precursors to secondary organic aerosol formation: acid-catalyzed reactive uptake studies with authentic compounds, *Environ. Sci. Technol.*, **46**, 250–258, doi:10.1021/es202554c, 2012.

Lin, Y.-H., Knipping, E. M., Edgerton, E. S., Shaw, S. L., and Surratt, J. D.: Investigating the influences of SO<sub>2</sub> and NH<sub>3</sub> levels on isoprene-derived secondary organic aerosol formation using conditional sampling approaches, *Atmos. Chem. Phys.*, **13**, 8457–8470, doi:10.5194/acp-13-8457-2013, 2013a.

Lin, Y., Zhang, H., Pye, H. O. T., Zhang, Z., Marth, W. J., Park, S., Arashiro, M., Cui, T., Budisulistorini, S. H., Sexton, K. G., Vizuete, W., Xie, Y., Luecken, D. J., Piletic, I. R., Edney, E. O., Bartolotti, L. J., Gold, A., and Surratt, J. D.: Epoxide as a precursor to secondary organic aerosol formation from isoprene photooxidation in the presence of nitrogen oxides, *P. Natl. Acad. Sci. USA*, doi:10.1073/pnas.1221150110, 2013b.

Lin, Y., Budisulistorini, S. H., Chu, K., Siejack, R. A., Zhang, H., Riva, M., Zhang, Z., Gold, A., Kautzman, K. E., and Surratt, J. D.: Light-absorbing oligomer formation in secondary organic aerosol from reactive uptake of isoprene epoxydiols, *Environ. Sci. Technol.*, **48**, 12012–12021, doi:10.1021/es503142b, 2014.

Liu, Y. J., Herdinger-Blatt, I., McKinney, K. A., and Martin, S. T.: Production of methyl vinyl ketone and methacrolein via the hydroperoxyl pathway of isoprene oxidation, *Atmos. Chem. Phys.*, **13**, 5715–5730, doi:10.5194/acp-13-5715-2013, 2013.

Liu, Y., Kuwata, M., Strick, B. F., Thomson, R. J., Geiger, F. M., McKinney, K., and Martin, S. T.: Uptake of epoxydiol isomers accounts for half of the particle-phase material produced from isoprene photooxidation via the HO<sub>2</sub> pathway, *Environ. Sci. Technol.*, doi:10.1021/es5034298, 2014.

Mauderly, J. L. and Chow, J. C.: Health effects of organic aerosols, *Inhal. Toxicol.*, **20**, 257–288, doi:10.1080/08958370701866008, 2008.

McNeill, V. F., Woo, J. L., Kim, D. D., Schwier, A. N., Wannell, N. J., Sumner, A. J., and Barakat, J. M.: Aqueous-phase secondary organic aerosol and organosulfate forma-



---

**Examining the effects  
of anthropogenic  
emissions on  
isoprene-derived  
SOA formation**S. H. Budisulistiorini et al.

---

[Title Page](#)[Abstract](#)[Introduction](#)[Conclusions](#)[References](#)[Tables](#)[Figures](#)[◀](#)[▶](#)[◀](#)[▶](#)[Back](#)[Close](#)[Full Screen / Esc](#)[Printer-friendly Version](#)[Interactive Discussion](#)

- Paatero, P. and Tapper, U.: Positive matrix factorization: a non-negative factor model with optimal utilization of error estimates of data values, *Environmetrics*, 5, 111–126, doi:10.1002/env.3170050203, 1994.
- Paatero, P., Hopke, P. K., Song, X., and Ramadan, Z.: Understanding and controlling rotations in factor analytic models, *Chemometr. Intell. Lab.*, 60, 253–264, doi:10.1016/S0169-7439(01)00200-3, 2002.
- Pandis, S. N., Paulson, S. E., Seinfeld, J. H., and Flagan, R. C.: Aerosol formation in the photooxidation of isoprene and  $\beta$ -pinene, *Atmos. Environ.*, 25, 997–1008, doi:10.1016/0960-1686(91)90141-S, 1991.
- Pankow, J. F.: An absorption model of gas/particle partitioning of organic compounds in the atmosphere, *Atmos. Environ.*, 28, 185–188, doi:10.1016/1352-2310(94)90093-0, 1994.
- Paulot, F., Crounse, J. D., Kjaergaard, H. G., Kürten, A., St. Clair, J. M., Seinfeld, J. H., and Wennberg, P. O.: Unexpected epoxide formation in the gas-phase photooxidation of isoprene, *Science*, 325, 730–733, doi:10.1126/science.1172910, 2009.
- Pye, H. O. T., Pinder, R. W., Piletic, I. R., Xie, Y., Capps, S. L., Lin, Y., Surratt, J. D., Zhang, Z., Gold, A., Luecken, D. J., Hutzell, W. T., Jaoui, M., Offenberg, J. H., Kleindienst, T. E., Lewandowski, M., and Edney, E. O.: Epoxide pathways improve model predictions of isoprene markers and reveal key role of acidity in aerosol formation, *Environ. Sci. Technol.*, 47, 11056–11064, doi:10.1021/es402106h, 2013.
- Riedel, T. P., Lin, Y., Budisulistiorini, S. H., Gaston, C. J., Thornton, J. A., Zhang, Z., Vizuete, W., Gold, A., and Surratt, J. D.: Heterogeneous reactions of isoprene-derived epoxides: reaction probabilities and molar secondary organic aerosol yield estimates, *Environ. Sci. Technol. Lett.*, doi:10.1021/ez500406f, 2015.
- Robinson, N. H., Hamilton, J. F., Allan, J. D., Langford, B., Oram, D. E., Chen, Q., Docherty, K., Farmer, D. K., Jimenez, J. L., Ward, M. W., Hewitt, C. N., Barley, M. H., Jenkin, M. E., Rickard, A. R., Martin, S. T., McFiggans, G., and Coe, H.: Evidence for a significant proportion of Secondary Organic Aerosol from isoprene above a maritime tropical forest, *Atmos. Chem. Phys.*, 11, 1039–1050, doi:10.5194/acp-11-1039-2011, 2011.
- Schichtel, B. A., Malm, W. C., Bench, G., Fallon, S., McDade, C. E., Chow, J. C., and Watson, J. G.: Fossil and contemporary fine particulate carbon fractions at 12 rural and urban sites in the United States, *J. Geophys. Res.*, 113, D02311, doi:10.1029/2007JD008605, 2008.

---

## Examining the effects of anthropogenic emissions on isoprene-derived SOA formation

S. H. Budisulistiorini et al.

---

[Title Page](#)[Abstract](#)[Introduction](#)[Conclusions](#)[References](#)[Tables](#)[Figures](#)[◀](#)[▶](#)[◀](#)[▶](#)[Back](#)[Close](#)[Full Screen / Esc](#)[Printer-friendly Version](#)[Interactive Discussion](#)

- Schwartz, S.: Mass-transport considerations pertinent to aqueous phase reactions of gases in liquid-water clouds, 6, 415–471, doi:10.1007/978-3-642-70627-1\_16, 1986.
- Slowik, J. G., Brook, J., Chang, R. Y.-W., Evans, G. J., Hayden, K., Jeong, C.-H., Li, S.-M., Liggio, J., Liu, P. S. K., McGuire, M., Mihele, C., Sjostedt, S., Vlasenko, A., and Abbatt, J. P. D.: Photochemical processing of organic aerosol at nearby continental sites: contrast between urban plumes and regional aerosol, *Atmos. Chem. Phys.*, 11, 2991–3006, doi:10.5194/acp-11-2991-2011, 2011.
- Sun, Y., Zhang, Q., Zheng, M., Ding, X., Edgerton, E. S., and Wang, X.: Characterization and source apportionment of water-soluble organic matter in atmospheric fine particles (PM<sub>2.5</sub>) with high-resolution aerosol mass spectrometry and GC-MS, *Environ. Sci. Technol.*, 45, 4854–4861, doi:10.1021/es200162h, 2011.
- Surratt, J. D., Murphy, S. M., Kroll, J. H., Ng, N. L., Hildebrandt, L., Sorooshian, A., Szmigielski, R., Vermeylen, R., Maenhaut, W., Claeys, M., Flagan, R. C., and Seinfeld, J. H.: Chemical composition of secondary organic aerosol formed from the photooxidation of isoprene, *J. Phys. Chem. A*, 110, 9665–9690, doi:10.1021/jp061734m, 2006.
- Surratt, J. D., Kroll, J. H., Kleindienst, T. E., Edney, E. O., Claeys, M., Sorooshian, A., Ng, N. L., Offenberg, J. H., Lewandowski, M., Jaoui, M., Flagan, R. C., and Seinfeld, J. H.: Evidence for organosulfates in secondary organic aerosol, *Environ. Sci. Technol.*, 41, 517–527, doi:10.1021/es062081q, 2007a.
- Surratt, J. D., Lewandowski, M., Offenberg, J. H., Jaoui, M., Kleindienst, T. E., Edney, E. O., and Seinfeld, J. H.: Effect of acidity on secondary organic aerosol formation from isoprene, *Environ. Sci. Technol.*, 41, 5363–5369, doi:10.1021/es0704176, 2007b.
- Surratt, J. D., Gómez-González, Y., Chan, A. W. H., Vermeylen, R., Shahgholi, M., Kleindienst, T. E., Edney, E. O., Offenberg, J. H., Lewandowski, M., Jaoui, M., Maenhaut, W., Claeys, M., Flagan, R. C., and Seinfeld, J. H.: Organosulfate formation in biogenic secondary organic aerosol, *J. Phys. Chem. A*, 112, 8345–8378, doi:10.1021/jp802310p, 2008.
- Surratt, J. D., Chan, A. W. H., Eddingsaas, N. C., Chan, M., Loza, C. L., Kwan, A. J., Hersey, S. P., Flagan, R. C., Wennberg, P. O., and Seinfeld, J. H.: Reactive intermediates revealed in secondary organic aerosol formation from isoprene, *P. Natl. Acad. Sci. USA*, 107, 6640–6645, doi:10.1073/pnas.0911114107, 2010.
- Tanner, R. L., Parkhurst, W. J., and McNichol, A. P.: Fossil sources of ambient aerosol carbon based on <sup>14</sup>C measurements special issue of aerosol science and technology on find-

## Examining the effects of anthropogenic emissions on isoprene-derived SOA formation

S. H. Budisulistiorini et al.

Title Page

Abstract

Introduction

Conclusions

References

Tables

Figures

◀

▶

◀

▶

Back

Close

Full Screen / Esc

Printer-friendly Version

Interactive Discussion

ings from the fine particulate matter supersites program, *Aerosol Sci. Tech.*, 38, 133–139, doi:10.1080/02786820390229453, 2004.

Tanner, R. L., Bairai, S. T., Olszyna, K. J., Valente, M. L., and Valente, R. J.: Diurnal patterns in PM<sub>2.5</sub> mass and composition at a background, complex terrain site, *Atmos. Environ.*, 39, 3865–3875, doi:10.1016/j.atmosenv.2005.03.014, 2005.

Tolocka, M. P., Jang, M., Ginter, J. M., Cox, F. J., Kamens, R. M., and Johnston, M. V.: Formation of oligomers in secondary organic aerosol, *Environ. Sci. Technol.*, 38, 1428–1434, doi:10.1021/es035030r, 2004.

Turpin, B. J. and Lim, H. J.: Species contributions to PM<sub>2.5</sub> mass concentrations: revisiting common assumptions for estimating organic mass, *Aerosol Sci. Tech.*, 35, 602–610, doi:10.1080/02786820119445, 2001.

Ulbrich, I. M., Canagaratna, M. R., Zhang, Q., Worsnop, D. R., and Jimenez, J. L.: Interpretation of organic components from Positive Matrix Factorization of aerosol mass spectrometric data, *Atmos. Chem. Phys.*, 9, 2891–2918, doi:10.5194/acp-9-2891-2009, 2009.

Veres, P., Roberts, J. M., Warneke, C., Welsh-Bon, D., Zahniser, M., Herndon, S., Fall, R., and de Gouw, J.: Development of negative-ion proton-transfer chemical-ionization mass spectrometry (NI-PT-CIMS) for the measurement of gas-phase organic acids in the atmosphere, *Int. J. Mass Spectrom.*, 274, 48–55, doi:10.1016/j.ijms.2008.04.032, 2008.

Wang, W., Kourtchev, I., Graham, B., Cafmeyer, J., Maenhaut, W., and Claeys, M.: Characterization of oxygenated derivatives of isoprene related to 2-methyltetrols in Amazonian aerosols using trimethylsilylation and gas chromatography/ion trap mass spectrometry, *Rapid Commun. Mass Sp.*, 19, 1343–1351, doi:10.1002/rcm.1940, 2005.

Woo, J. L. and McNeill, V. F.: simpleGAMMA – a reduced model of secondary organic aerosol formation in the aqueous aerosol phase (aaSOA), *Geosci. Model Dev. Discuss.*, 8, 463–482, doi:10.5194/gmdd-8-463-2015, 2015.

Worton, D. R., Surratt, J. D., LaFranchi, B. W., Chan, A. W. H., Zhao, Y., Weber, R. J., Park, J., Gilman, J. B., de Gouw, J., Park, C., Schade, G., Beaver, M., Clair, J. M. S., Crouse, J., Wennberg, P., Wolfe, G. M., Harrold, S., Thornton, J. A., Farmer, D. K., Docherty, K. S., Cubison, M. J., Jimenez, J., Frossard, A. A., Russell, L. M., Kristensen, K., Glasius, M., Mao, J., Ren, X., Brune, W., Browne, E. C., Pusede, S. E., Cohen, R. C., Seinfeld, J. H., and Goldstein, A. H.: Observational insights into aerosol formation from isoprene, *Environ. Sci. Technol.*, 47, 11403–11413, doi:10.1021/es4011064, 2013.

---

**Examining the effects  
of anthropogenic  
emissions on  
isoprene-derived  
SOA formation**S. H. Budisulistiorini et al.

---

[Title Page](#)[Abstract](#)[Introduction](#)[Conclusions](#)[References](#)[Tables](#)[Figures](#)[◀](#)[▶](#)[◀](#)[▶](#)[Back](#)[Close](#)[Full Screen / Esc](#)[Printer-friendly Version](#)[Interactive Discussion](#)

- Xu, L., Guo, H., Boyd, C. M., Klein, M., Bougiatioti, A., Cerully, K. M., Hite, J. R., Isaacman-VanWertz, G., Kreisberg, N. M., Knote, C., Olson, K., Koss, A., Goldstein, A. H., Hering, S. V., de Gouw, J., Baumann, K., Lee, S., Nenes, A., Weber, R. J., and Ng, N. L.: Effects of anthropogenic emissions on aerosol formation from isoprene and monoterpenes in the south-eastern United States, *P. Natl. Acad. Sci. USA*, 112, 37–42, doi:10.1073/pnas.1417609112, 2015.
- Zhang, H., Surratt, J. D., Lin, Y. H., Bapat, J., and Kamens, R. M.: Effect of relative humidity on SOA formation from isoprene/NO photooxidation: enhancement of 2-methylglyceric acid and its corresponding oligoesters under dry conditions, *Atmos. Chem. Phys.*, 11, 6411–6424, doi:10.5194/acp-11-6411-2011, 2011.
- Zhang, Q. Q.: Understanding atmospheric organic aerosols via factor analysis of aerosol mass spectrometry: a review, *Anal. Bioanal. Chem.*, 401, 3045–3067, 2011.
- Zhang, X., Liu, Z., Hecobian, A., Zheng, M., Frank, N. H., Edgerton, E. S., and Weber, R. J.: Spatial and seasonal variations of fine particle water-soluble organic carbon (WSOC) over the southeastern United States: implications for secondary organic aerosol formation, *Atmos. Chem. Phys.*, 12, 6593–6607, doi:10.5194/acp-12-6593-2012, 2012a.
- Zhang, Z., Lin, Y.-H., Zhang, H., Surratt, J. D., Ball, L. M., and Gold, A.: Technical Note: Synthesis of isoprene atmospheric oxidation products: isomeric epoxydiols and the rearrangement products cis- and trans-3-methyl-3,4-dihydroxytetrahydrofuran, *Atmos. Chem. Phys.*, 12, 8529–8535, doi:10.5194/acp-12-8529-2012, 2012b.

## Examining the effects of anthropogenic emissions on isoprene-derived SOA formation

S. H. Budisulistiorini et al.

Title Page

Abstract

Introduction

Conclusions

References

Tables

Figures

◀

▶

◀

▶

Back

Close

Full Screen / Esc

Printer-friendly Version

Interactive Discussion

**Table 1.** Summary of isoprene-derived SOA tracers measured by GC/EI-MS and UPLC/DAD-ESI-HR-QTOFMS.

SOA Tracers	Retention Time (min)	# of Samples Detected <sup>a</sup>	Concentration (ng m <sup>-3</sup> )		Average % among detected tracers
			Maximum	Mean	
<b>Tracers by GC/EI-MS</b>					
<i>trans</i> -3-MeTHF-3,4-diol	20.5	55	18.8	2.7	0.6 %
<i>cis</i> -3-MeTHF-3,4-diol	21.1	29	5.7	1.7	0.4 %
2-methylglyceric acid	23.4	119	36.7	7.5	1.6 %
2-methylthreitol	32.9	122	329.8	42.4	9.2 %
2-methylerythritol	33.7	122	1269.7	120.7	26.3 %
(Z)-2-methylbut-3-ene-1,2,4-triol	25.6	121	260.0	29.1	6.1 %
2-methylbut-3-ene-1,2,3-triol	26.6	118	162.5	16.5	3.6 %
(E)-2-methylbut-3-ene-1,2,4-triol	26.9	122	1127.0	98.8	21.5 %
<b>Tracers by UPLC/DAD-ESI-HR-QTOFMS tracers</b>					
IEPOX-derived organosulfates	1.1–1.7	122	835.3	139.2	30.3 %
IEPOX-derived organosulfate dimer	2.8	103	10.3	1.1	0.2 %
MAE-derived organosulfate	1.1	114	57.3	8.2	1.8 %

<sup>a</sup> Total number of samples is 123.

## Examining the effects of anthropogenic emissions on isoprene-derived SOA formation

S. H. Budisulistiorini et al.

**Table 2.** Correlation ( $r^2$ ) of PMF Factors with isoprene-derived SOA tracers measured by GC/EI-MS and UPLC/DAD-ESI-HR-QTOFMS.

SOA Tracers	IEPOX-OA	LV-OOA	91Fac
3-methyltetrahydrofuran-3,4-diols	0.12	0.13	0.24
2-methyltetrols	0.80	0.20	0.38
C <sub>5</sub> -alkene triols	0.75	0.19	0.44
2-methylglyceric acids	0.38	0.44	0.44
IEPOX-derived organosulfates	0.81	0.32	0.42
IEPOX-derived dimer organosulfate	0.73	0.11	0.34
MAE-derived organosulfate	0.45	0.47	0.51

Title Page

Abstract

Introduction

Conclusions

References

Tables

Figures

◀

▶

◀

▶

Back

Close

Full Screen / Esc

Printer-friendly Version

Interactive Discussion



## Examining the effects of anthropogenic emissions on isoprene-derived SOA formation

S. H. Budisulistiorini et al.

Title Page

Abstract

Introduction

Conclusions

References

Tables

Figures

◀

▶

◀

▶

Back

Close

Full Screen / Esc

Printer-friendly Version

Interactive Discussion



**Table 3.** Correlation ( $r^2$ ) of modeled SOA tracers with measurements.

$H^*$ ( $\text{M atm}^{-1}$ )	2-methyltetrols		IEPOX organosulfates	
	$r^2$	Slope	$r^2$	Slope
$3.0 \times 10^7$ <sup>a</sup>	0.45	$9.61 \pm 0.91$	0.66	$11.70 \pm 0.81$
$2.7 \times 10^6$ <sup>b</sup>	0.44	$0.69 \pm 0.06$	0.66	$0.99 \pm 0.07$

<sup>a</sup> Nguyen et al. (2014).

<sup>b</sup> Pye et al. (2013).

## Examining the effects of anthropogenic emissions on isoprene-derived SOA formation

S. H. Budisulistiorini et al.

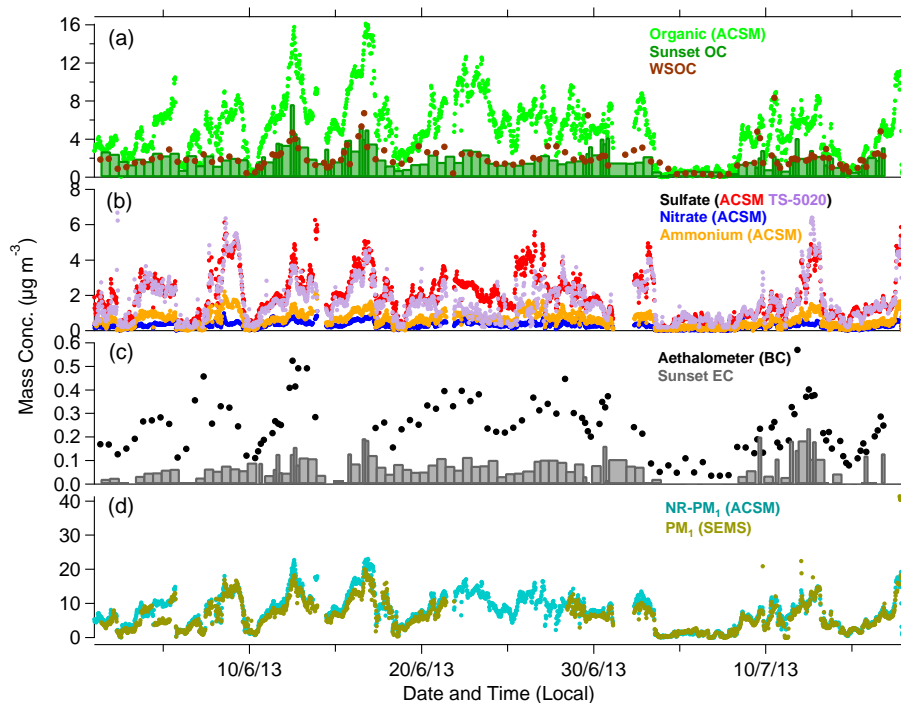


**Figure 1.** Time series mass concentration of **(a)** organic and **(b)** inorganics (excluding chloride) measured by ACSM, **(c)** black carbon (BC) measured by Aethalometer, and **(d)** NR-PM<sub>1</sub> and PM<sub>1</sub> mass concentrations measured by ACSM and SEMS-MCPC. Collocated sulfate aerosol measured by Thermo Scientific Sulfate Analyzer was plotted on **(b)**. OC (bars) and WSOC (dots), both in unit of  $\mu\text{gCm}^{-3}$ , measured from filter samples were plotted on **(a)** with ACSM organic. EC (bars; in unit of  $\mu\text{gCm}^{-3}$ ) measured from filter samples were plotted on **(c)** along with BC measurements.

## Examining the effects of anthropogenic emissions on isoprene-derived SOA formation

S. H. Budisulistiorini et al.

Title Page

Abstract

Introduction

Conclusions

References

Tables

Figures

◀

▶

◀

▶

Back

Close

Full Screen / Esc

Printer-friendly Version

Interactive Discussion

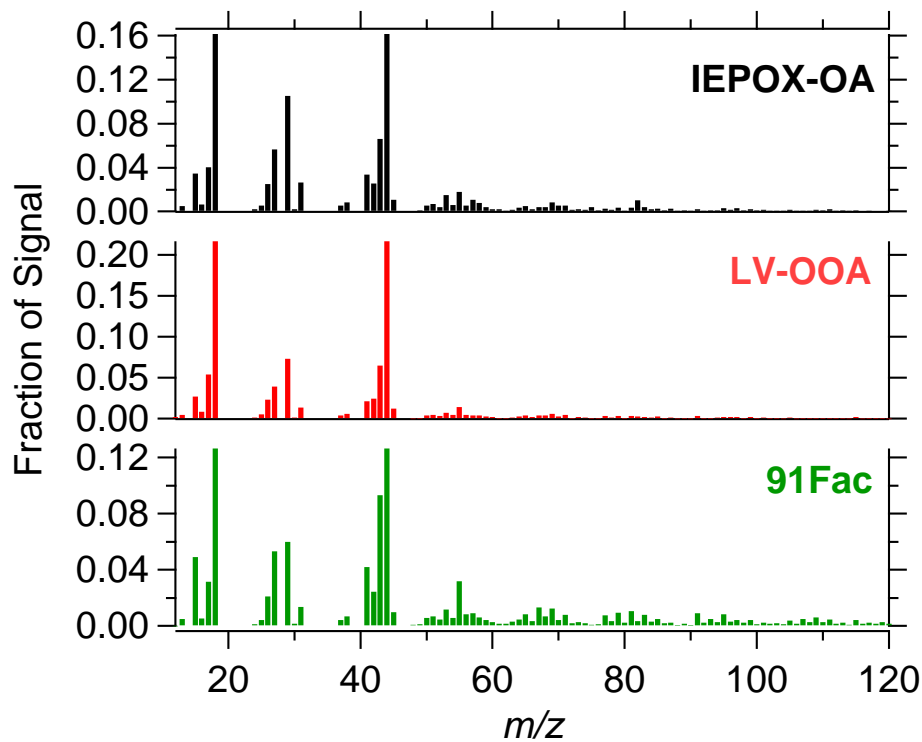


**Figure 2.** Mass spectra obtained for the 3 factor solution from PMF: IEPOX-OA, LV-OOA, and 91Fac.

## Examining the effects of anthropogenic emissions on isoprene-derived SOA formation

S. H. Budisulistiorini et al.

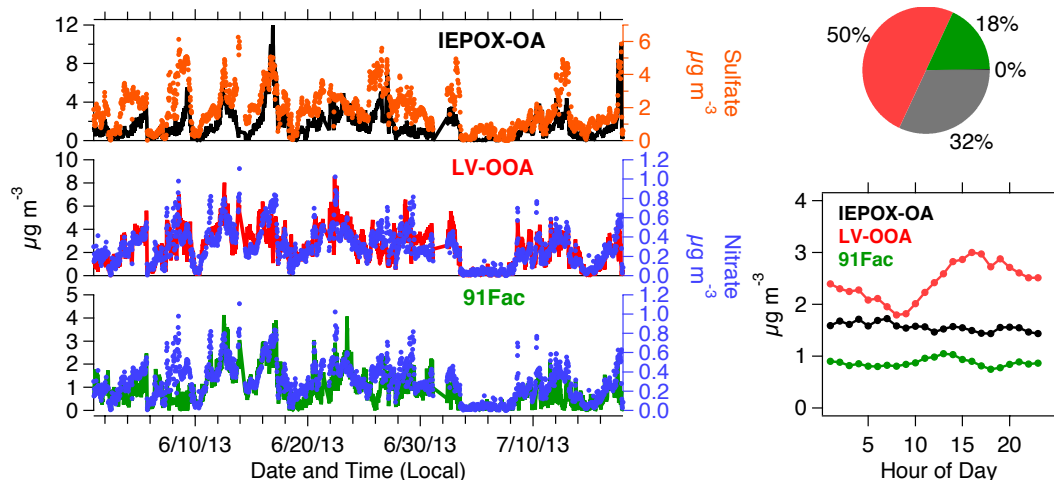


**Figure 3.** Left panel shows the PMF 3 factor solution time series mass contributions measured by ACSM. Top to bottom: left ordinate, IEPOX-OA (black), LV-OOA (red), and 91Fac (green); right ordinate, sulfate (orange) and nitrate (blue). Right panel shows average mass contributions (top) and diurnal variation (bottom) of factors resolved by PMF.

## Examining the effects of anthropogenic emissions on isoprene-derived SOA formation

S. H. Budisulistiorini et al.

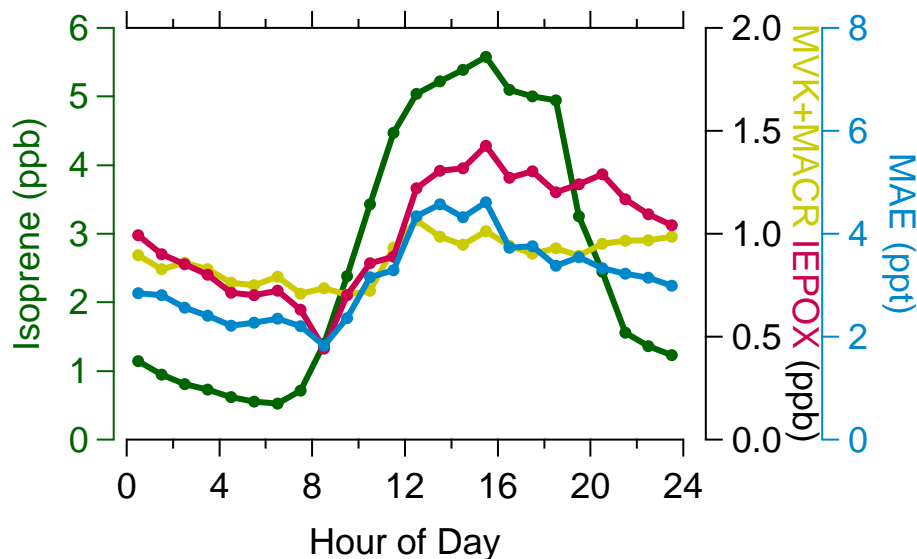


**Figure 4.** Diurnal variation of isoprene (left ordinate) as well as isoprene gaseous 3 photooxidation products (right ordinates), i.e., MVK + MACR, IEPOX and MAE, measured at LRK site. It should be noted that IEPOX signal includes interference of ISOPOOH at unknown ratio, thus its mixing ratio represents an upper limit.

Title Page	
Abstract	Introduction
Conclusions	References
Tables	Figures
◀	▶
◀	▶
Back	Close
Full Screen / Esc	
Printer-friendly Version	
Interactive Discussion	

## Examining the effects of anthropogenic emissions on isoprene-derived SOA formation

S. H. Budisulistiorini et al.

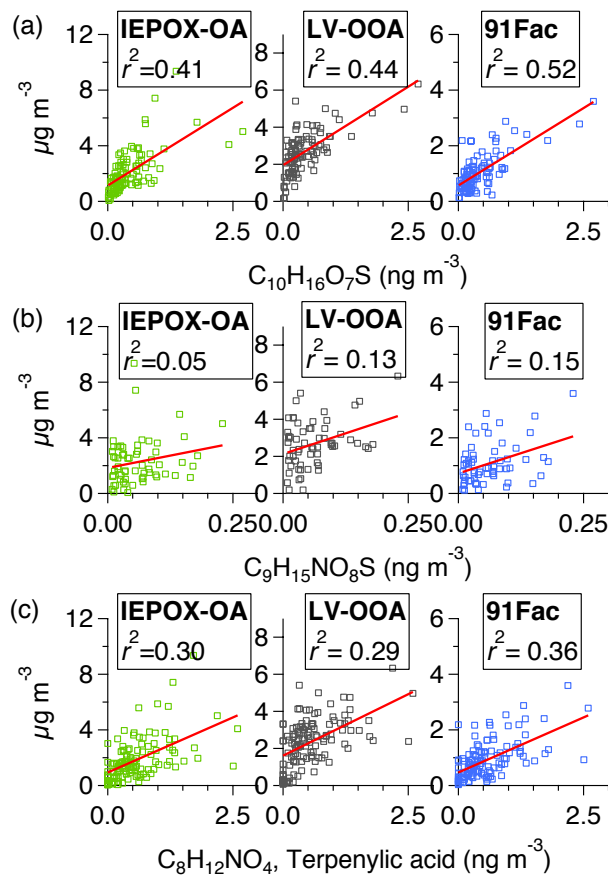


**Figure 5.** Correlation of PMF factors with  $\alpha$ -pinene derived organosulfate,  $\text{C}_{10}\text{H}_{16}\text{O}_7\text{S}$  (a), nitrated organosulfates,  $\text{C}_9\text{H}_{15}\text{NO}_8\text{S}$  (b), and terpenylic acid  $\text{C}_8\text{H}_{12}\text{NO}_4$  (c).

[Title Page](#)
[Abstract](#)
[Introduction](#)
[Conclusions](#)
[References](#)
[Tables](#)
[Figures](#)
[Back](#)
[Close](#)
[Full Screen / Esc](#)
[Printer-friendly Version](#)
[Interactive Discussion](#)

## Examining the effects of anthropogenic emissions on isoprene-derived SOA formation

S. H. Budisulistiorini et al.

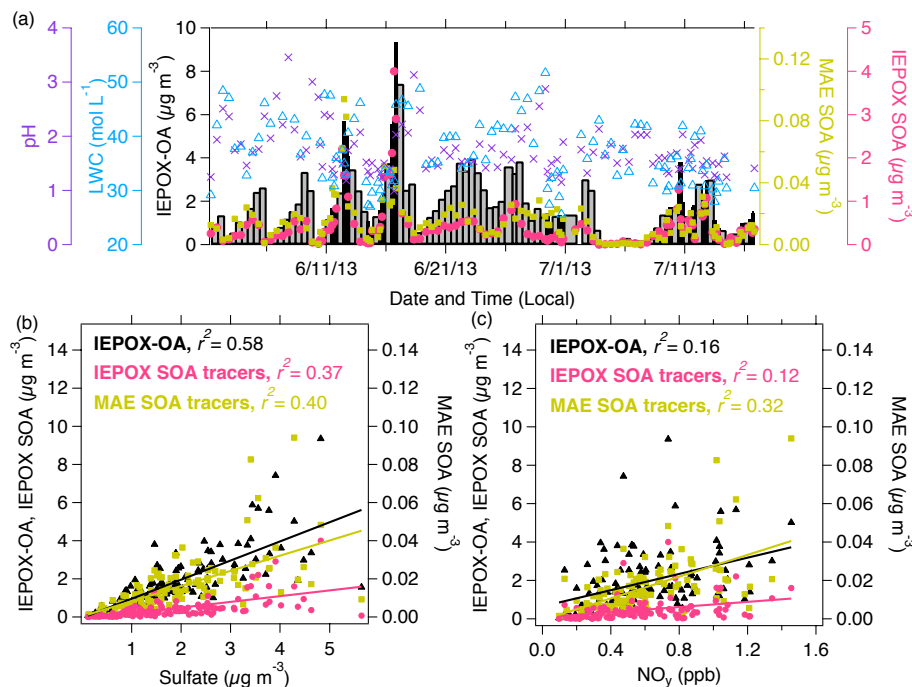


**Figure 6.** (a) Time series of IEPOX-OA factor (black bars; darker bars are intensive filter sampling periods), sum of IEPOX-derived (pink circle) and MAE-derived (yellow square) SOA tracers, aerosol pH (purple cross) and LWC (blue triangle) estimated by ISORROPIA-II model. Campaign average pH and LWC are  $1.78 \pm 0.53$  and  $38.71 \pm 7.43 \text{ mol L}^{-1}$ , respectively. Correlation plots between IEPOX-OA, summed of IEPOX- and MAE-derived SOA tracers and (b) sulfate measurements by ACSM and (c) NO<sub>y</sub> measurements from NPS.

Title Page

Abstract

Introduction

Conclusions

References

Tables

Figures

◀

▶

◀

▶

Back

Close

Full Screen / Esc

Printer-friendly Version

Interactive Discussion

## Examining the effects of anthropogenic emissions on isoprene-derived SOA formation

S. H. Budisulistiorini et al.

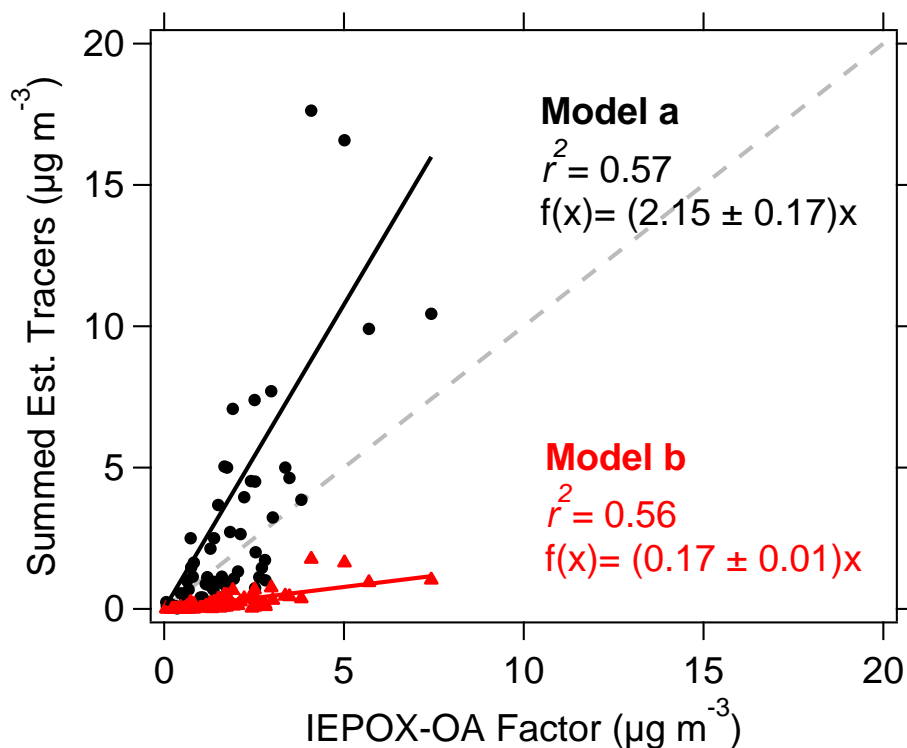


**Figure 7.** Correlation of summed IEPOX-derived SOA tracers estimated by simpleGAMMA by assuming  $H^*$  of  $3.0 \times 10^7$  (Nguyen et al., 2014) (model a) and  $2.7 \times 10^6$  (Pye et al., 2013) (model b) and IEPOX-OA factor from PMF analysis.

[Title Page](#)[Abstract](#)[Introduction](#)[Conclusions](#)[References](#)[Tables](#)[Figures](#)[◀](#)[▶](#)[◀](#)[▶](#)[Back](#)[Close](#)[Full Screen / Esc](#)[Printer-friendly Version](#)[Interactive Discussion](#)